Perception of images by the visual cortex: geometry in neuroscience

Pascal Chossat

"Dynamical and complex systems"

For the 60th birthday of Jean-Marc Gambaudo

UNIVERSITÉ CÔTE D'AZUR
cnrs
Inria INVENTEURS DU MONDE NUMÉRIQUE
Université Nice Sophia Antipolis

Vision processing by the brain: a complex system

How does the brain process input signal from the retina to give a global and as much as possible coherent representation of the outer world (the "Gestalt")?

Indeed, informations from retina $\longrightarrow$ visual cortex are essentially local...

Vision processing by the brain: a complex system

How does the brain process input signal from the retina to give a global and as much as possible coherent representation of the outer world (the "Gestalt")?

Indeed, informations from retina → visual cortex are essentially local...

Examples:

Illusory contours

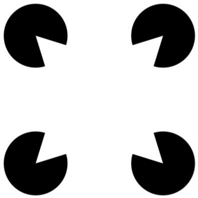

Vision processing by the brain: a complex system

How does the brain process input signal from the retina to give a global and as much as possible coherent representation of the outer world (the "Gestalt")?

Indeed, informations from retina $\longrightarrow$ visual cortex are essentially local...

Examples:

Illusory contours

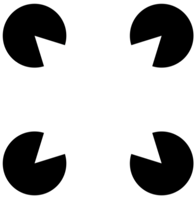

Visual hallucinations

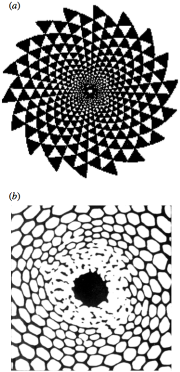

Outline of the talk

Outline of the talk

1. Functional architecture of the primary visual cortex.
   - rough sketch of the best studied feature detected by the visual cortex and its geometrical interpretation: contour detection.
   - much more detailed and extended presentation is the book by Jean Petitot *Elements of Neurogeometry*, Springer 2017.

Outline of the talk

1. Functional architecture of the primary visual cortex.
   - rough sketch of the best studied feature detected by the visual cortex and its geometrical interpretation: contour detection.
   - much more detailed and extended presentation is the book by Jean Petitot *Elements of Neurogeometry*, Springer 2017.
2. Application to the spontaneous activity of the primary visual cortex (geometric hallucinations).
   A quick overview of the theory by Paul Bressloff et al (2000).

Outline of the talk

1. Functional architecture of the primary visual cortex.
   - rough sketch of the best studied feature detected by the visual cortex and its geometrical interpretation: contour detection.
   - much more detailed and extended presentation is the book by Jean Petitot *Elements of Neurogeometry*, Springer 2017.
2. Application to the spontaneous activity of the primary visual cortex (geometric hallucinations).
   A quick overview of the theory by Paul Bressloff et al (2000).
3. Extending 1 and 2 to more features: the "hyperbolic" model.
   A recent attempt to incorporate more features to the ring model by replacing "orientation" with "structure tensor" (Gregory Faye's thesis, Inria 2013) $\rightarrow$ pattern formation problem in the hyperbolic plane.

The neuron, basic unit of the cortical complex system

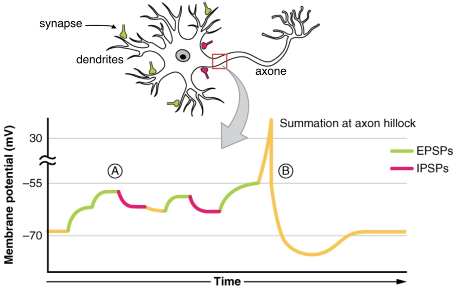

- Neurons are active units, which emit spike trains along axon when input exceeds a threshold

- Synapses are either excitatory (green) or inhibitory (red)

The neuron, basic unit of the cortical complex system

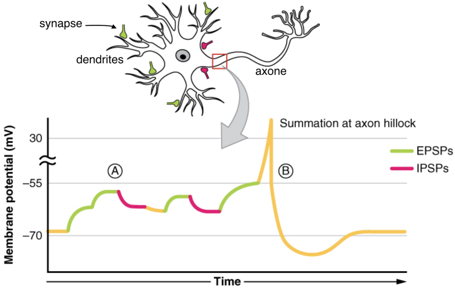

- Neurons are active units, which emit spike trains along axon when input exceeds a threshold

- Synapses are either excitatory (green) or inhibitory (red)

- In a specific brain area there are millions of neurons.

The neuron, basic unit of the cortical complex system

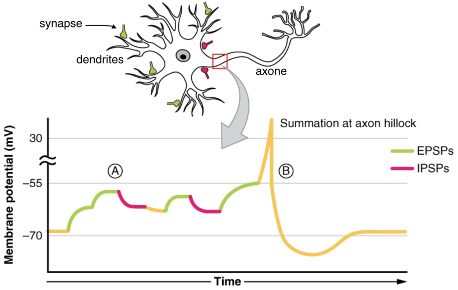

- Neurons are active units, which emit spike trains along axon when input exceeds a threshold

- Synapses are either excitatory (green) or inhibitory (red)

- In a specific brain area there are millions of neurons.
- It is relevant to consider space and time averages of the activity $\rightarrow$ continuous time evolution of neural fields (as measured in ECG, FMRI). Then "neuron" means in fact "population of neurons".

The neuron, basic unit of the cortical complex system

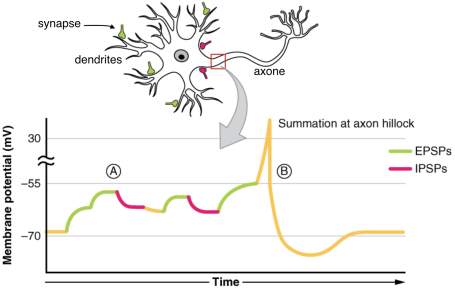

- Neurons are active units, which emit spike trains along axon when input exceeds a threshold

- Synapses are either excitatory (green) or inhibitory (red)

- In a specific brain area there are millions of neurons.
- It is relevant to consider space and time averages of the activity $\rightarrow$ continuous time evolution of neural fields (as measured in ECG, FMRI). Then "neuron" means in fact "population of neurons".
- Synaptic plasticity allows reconfiguration of circuitry at various time scales (long-term and short-term learning, adaptation..).

Global structure of the visual cortex in primates

Global structure of the visual cortex in primates

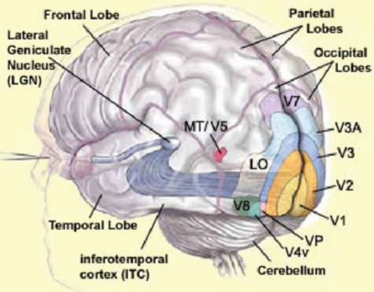

Signal generated on retina is transmitted to the primary visual area $V1$ after filtering (smoothing) in the LGN.
Then forwarded to other areas $V2$, $V3$...

Global structure of the visual cortex in primates

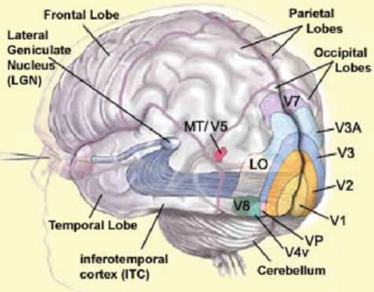

Signal generated on retina is transmitted to the primary visual area $V1$ after filtering (smoothing) in the LGN. Then forwarded to other areas $V2$, $V3$...

Each neuron in $V1$ responds to a local receptive field in the visual field VF where it detects orientation, contrast, spatial frequency, ocular dominance...

Global structure of the visual cortex in primates

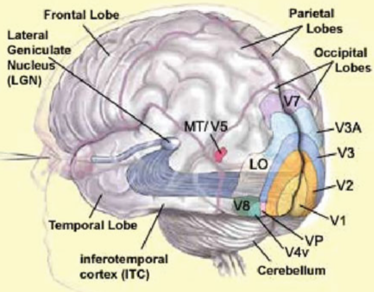

Signal generated on retina is transmitted to the primary visual area $V1$ after filtering (smoothing) in the LGN.
Then forwarded to other areas $V2$, $V3$...

Each neuron in $V1$ responds to a local receptive field in the visual field VF where it detects orientation, contrast, spatial frequency, ocular dominance...

Typical receptive profile φ of a neuron in $V1$:

It filters the signal $I(x,y)$ at a spatial scale with a local orientation: $I_\varphi = I * \varphi$ (for example $\varphi = \partial_x^2 G$, $G(x,y)$ Gauss function).

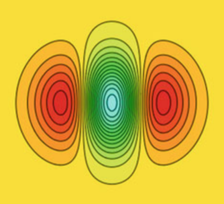

Retinotopy

Small patches in the visual field VF are mapped to small patches in $V1$ according to a roughly $\log(z)$ law ($z \in \mathbb{C} \simeq$ VF).

This retinotopic map $VF \to V1$ is an approximately conformal map. The fovea is mapped to a large domain in $V1$.

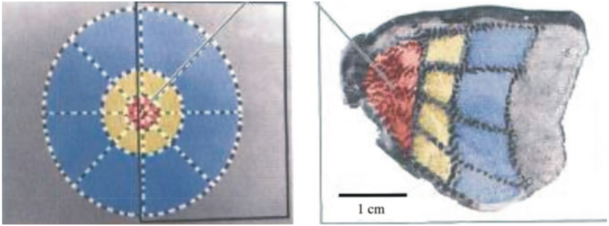

Retinotopic map for a macaque

Columnar stucture of V1 (Hubel & Wiesel 1960's)

Columnar stucture of V1 (Hubel & Wiesel 1960's)

1. They got the Nobel prize in physiology (1981) for this discovery..

Columnar stucture of V1 (Hubel & Wiesel 1960's)

1. They got the Nobel prize in physiology (1981) for this discovery..
2. $V1$ is composed of six "horizontal" layers. Experiments show:

- Neurons in a vertical column detect the same orientation, except at singular columns called pinwheels where all orientations are present.
- Neurons in adjacent columns detect different orientations by steps of $\sim 10^\circ$.

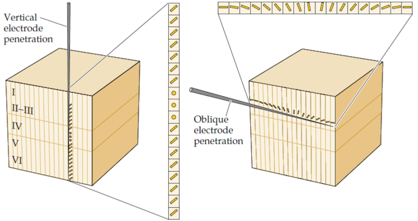

Columnar stucture of V1 (Hubel & Wiesel 1960's)

1. They got the Nobel prize in physiology (1981) for this discovery..
2. $V1$ is composed of six "horizontal" layers. Experiments show:

- Neurons in a vertical column detect the same orientation, except at singular columns called pinwheels where all orientations are present.
- Neurons in adjacent columns detect different orientations by steps of $\sim 10^\circ$.

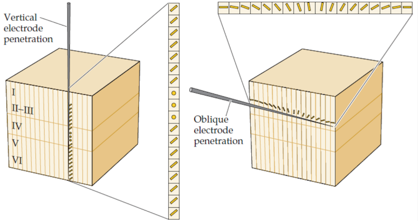

3. The patch of adjacent columns surrounding a pinwheel defines a hypercolumn ($\sim 0.6mm^2$), in which neurons respond to the same location in retina but to different orientations.

Columnar stucture of V1 (Hubel & Wiesel 1960's)

1. They got the Nobel prize in physiology (1981) for this discovery..
2. $V1$ is composed of six "horizontal" layers. Experiments show:

- Neurons in a vertical column detect the same orientation, except at singular columns called pinwheels where all orientations are present.
- Neurons in adjacent columns detect different orientations by steps of $\sim 10^\circ$.

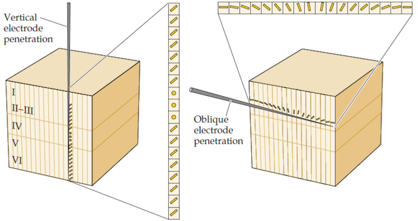

3. The patch of adjacent columns surrounding a pinwheel defines a hypercolumn ($\sim 0.6mm^2$), in which neurons respond to the same location in retina but to different orientations.
4. Other features are engrafted in hypercolumns: contrast, spatial frequency, ocular dominance, that could be accounted for as well.

Hypercolumnar crystalline structure of $V1$

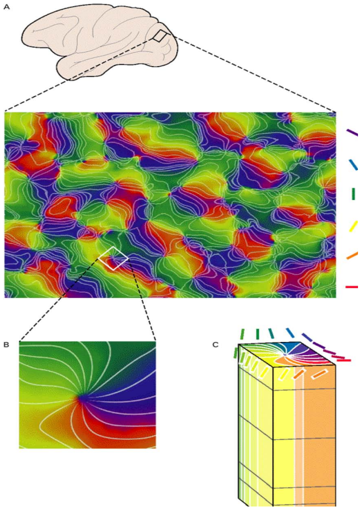

Hypercolumnar crystalline structure of $V1$

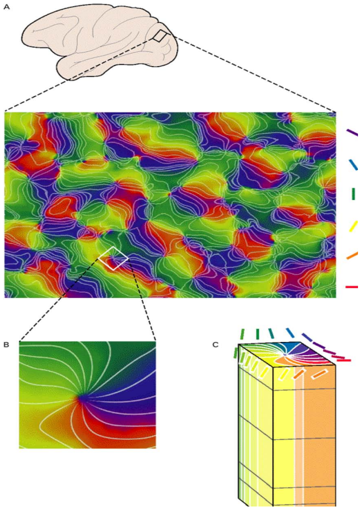

(i) Diametrically opposite rays correspond to orientations differing by $\pi/2$.

Hypercolumnar crystalline structure of $V1$

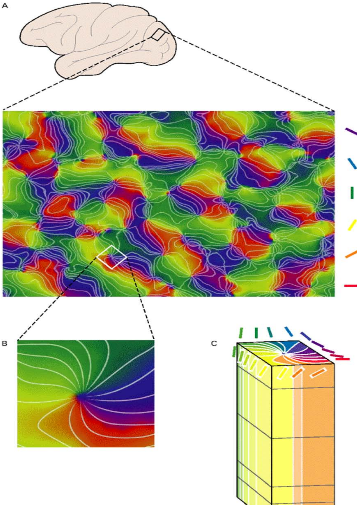

(i) Diametrically opposite rays correspond to orientations differing by $\pi/2$.

(ii) Pinwheels form a crystal lattice on $V1$.

Hypercolumnar crystalline structure of $V1$

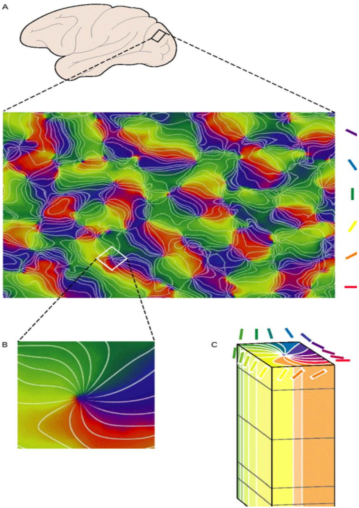

(i) Diametrically opposite rays correspond to orientations differing by $\pi/2$.

(ii) Pinwheels form a crystal lattice on $V1$.

(iii) Iso-orientation lines define a field of orientations, of which pinwheels are singular points.

Hypercolumnar crystalline structure of $V1$

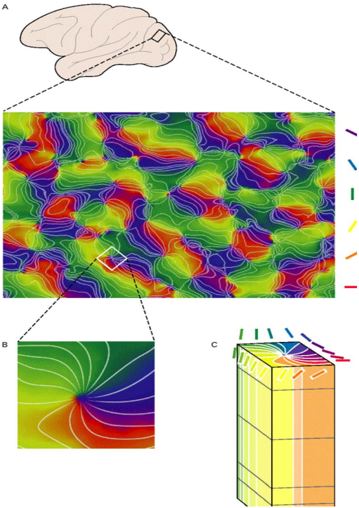

(i) Diametrically opposite rays correspond to orientations differing by $\pi/2$.

(ii) Pinwheels form a crystal lattice on $V1$.

(iii) Iso-orientation lines define a field of orientations, of which pinwheels are singular points.

(iv) Tempting to idealize the hypercolumnar structure by a fiber bundle structure $R \times \mathbb{P}^1$: R = retinal field (base plane) and fiber = set of orientations $\simeq$ projective line.

This can be justified to some extent by blowing-up the pinwheel singularities (see Petitot's book)

The fiber bundle $V1$ as an efficient detector of contours

The fiber bundle $V1$ as an efficient detector of contours

- Let γ be a curve in $R \simeq \mathbb{R}^2$ with tangent angle θ at (x, y).
  γ lifts to the curve $\Gamma = \{(x, y, \theta)\}$ in $R \times \mathbb{P}^1 \simeq R \times \mathbb{S}^1$ $(\theta \in [0, \pi))$.

  This allows to replace the evaluation of dy/dx at each $(x, y) \in \gamma$ by the selection of a point in the fiber bundle: much more efficient!

The fiber bundle $V1$ as an efficient detector of contours

- Let γ be a curve in $R \simeq \mathbb{R}^2$ with tangent angle θ at (x, y).
  γ lifts to the curve $\Gamma = \{(x, y, \theta)\}$ in $R \times \mathbb{P}^1 \simeq R \times \mathbb{S}^1$ $(\theta \in [0, \pi))$.

  This allows to replace the evaluation of dy/dx at each $(x, y) \in \gamma$ by the selection of a point in the fiber bundle: much more efficient!
- Γ is the lift of a curve in R if any tangent vector to Γ belongs to the kernel of the differential 1-form $\omega = \cos(\theta)dy - \sin(\theta)dx$.
- $\ker \omega$ defines a distribution of planes (called horizontal) in $T(R \times \mathbb{S}^1)$, spanned at each point (x, y, θ) by $\cos(\theta)\partial_x + \sin(\theta)\partial_y$ and ∂_θ.

The fiber bundle $V1$ as an efficient detector of contours

- Let γ be a curve in $R \simeq \mathbb{R}^2$ with tangent angle θ at (x, y). γ lifts to the curve $\Gamma = \{(x, y, \theta)\}$ in $R \times \mathbb{P}^1 \simeq R \times \mathbb{S}^1$ $(\theta \in [0, \pi))$.

  This allows to replace the evaluation of dy/dx at each $(x, y) \in \gamma$ by the selection of a point in the fiber bundle: much more efficient!
- Γ is the lift of a curve in R if any tangent vector to Γ belongs to the kernel of the differential 1-form $\omega = \cos(\theta)dy - \sin(\theta)dx$.
- $\ker \omega$ defines a distribution of planes (called horizontal) in $T(R \times \mathbb{S}^1)$, spanned at each point (x, y, θ) by $\cos(\theta)\partial_x + \sin(\theta)\partial_y$ and ∂_θ.
- Note that this distribution of horizontal planes (contact structure) is not the enveloppe of a surface in $R \times \mathbb{S}^1$ (it dos not satisfy Froebenius condition $\omega \wedge d\omega = 0$). It is devoted to path (contour) integration.

The fiber bundle $V1$ as an efficient detector of contours

- Let γ be a curve in $R \simeq \mathbb{R}^2$ with tangent angle θ at (x, y).
  γ lifts to the curve $\Gamma = \{(x, y, \theta)\}$ in $R \times \mathbb{P}^1 \simeq R \times \mathbb{S}^1$ $(\theta \in [0, \pi))$.
  This allows to replace the evaluation of dy/dx at each $(x, y) \in \gamma$ by the selection of a point in the fiber bundle: much more efficient!
- Γ is the lift of a curve in R if any tangent vector to Γ belongs to the kernel of the differential 1-form $\omega = \cos(\theta)dy - \sin(\theta)dx$.
- $\ker\omega$ defines a distribution of planes (called horizontal) in $T(R \times \mathbb{S}^1)$, spanned at each point (x, y, θ) by $\cos(\theta)\partial_x + \sin(\theta)\partial_y$ and ∂_θ.
- Note that this distribution of horizontal planes (contact structure) is not the enveloppe of a surface in $R \times \mathbb{S}^1$ (it dos not satisfy Froebenius condition $\omega \wedge d\omega = 0$). It is devoted to path (contour) integration.

It is tempting to say that pinwheels and their iso-orientation rays represent a discrete neural implementation of this contact structure.

But how does the brain proceed to compare orientations at remote points in R?

Long-range horizontal connections in $V1$

Experiments show:
(i) Neurons with long-range axons connect preferentially to neurons with the same orientation in other hypercolumns.

Long-range horizontal connections in $V1$

Experiments show:
(i) Neurons with long-range axons connect preferentially to neurons with the same orientation in other hypercolumns.
(ii) Coaxiality: the path of connections tends to be aligned with orientation.

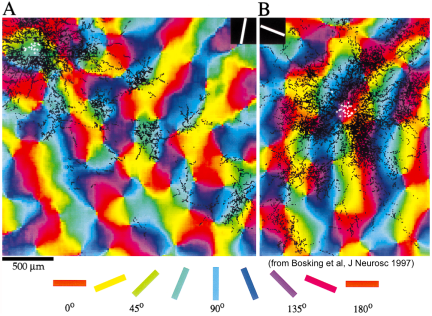

(from Bosking et al, J Neurosc 1997)

Long-range horizontal connections in $V1$

Experiments show:
(i) Neurons with long-range axons connect preferentially to neurons with the same orientation in other hypercolumns.
(ii) Coaxiality: the path of connections tends to be aligned with orientation.

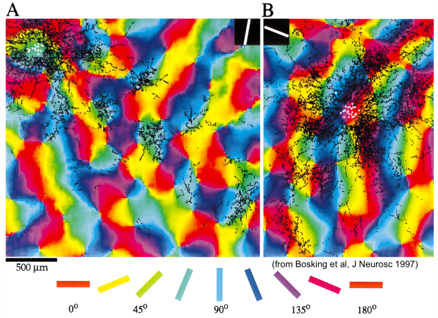

In contrast, note that within the hypercolumn the field of connections looks quite isotropic: it equally reaches all orientations.

$V1$ as the Lie group of displacements in the plane

- $SE(2) = \mathbb{R}^2 \ltimes SO(2)$ is the Lie group of rigid displacements in the plane, with product $(\mathbf{t}, r_\phi) \cdot (\mathbf{t}', r_{\phi'}) = (\mathbf{t} + r_\phi \mathbf{t}', r_{\phi+\phi'})$.

$V1$ as the Lie group of displacements in the plane

- $SE(2) = \mathbb{R}^2 \ltimes SO(2)$ is the Lie group of rigid displacements in the plane, with product $(\mathbf{t}, r_\phi) \cdot (\mathbf{t}', r_{\phi'}) = (\mathbf{t} + r_\phi \mathbf{t}', r_{\phi+\phi'})$.
- $SE(2)$ is the principal bundle associated with $R \times \mathbb{P}^1$: $\mathbb{R}^2 \simeq SE(2)/SO(2)$.

$V1$ as the Lie group of displacements in the plane

- $SE(2) = \mathbb{R}^2 \ltimes SO(2)$ is the Lie group of rigid displacements in the plane, with product $(\mathbf{t}, r_\phi) \cdot (\mathbf{t}', r_{\phi'}) = (\mathbf{t} + r_\phi \mathbf{t}', r_{\phi+\phi'})$.
- $SE(2)$ is the principal bundle associated with $R \times \mathbb{P}^1$: $\mathbb{R}^2 \simeq SE(2)/SO(2)$.
- Then ω is invariant under the action of $SE(2)$ on $T(\mathbb{R}^2 \times SO(2))$: any two horizontal planes in $\mathbb{R}^2 \times SO(2)$ can be equivariantly identified by a suitable displacement.

  The distribution of horizontal planes realizes a connection in $R \times SO(2)$, allowing for parallel transport, covariant derivation...

$V1$ as the Lie group of displacements in the plane

- $SE(2) = \mathbb{R}^2 \ltimes SO(2)$ is the Lie group of rigid displacements in the plane, with product $(\mathbf{t}, r_\phi) \cdot (\mathbf{t}', r_{\phi'}) = (\mathbf{t} + r_\phi \mathbf{t}', r_{\phi+\phi'})$.
- $SE(2)$ is the principal bundle associated with $R \times \mathbb{P}^1$: $\mathbb{R}^2 \simeq SE(2)/SO(2)$.
- Then ω is invariant under the action of $SE(2)$ on $T(\mathbb{R}^2 \times SO(2))$: any two horizontal planes in $\mathbb{R}^2 \times SO(2)$ can be equivariantly identified by a suitable displacement.

  The distribution of horizontal planes realizes a connection in $R \times SO(2)$, allowing for parallel transport, covariant derivation...
- The long-range connections in $V1$ implement these contact structure and connection.

$V1$ as the Lie group of displacements in the plane

- $SE(2) = \mathbb{R}^2 \ltimes SO(2)$ is the Lie group of rigid displacements in the plane, with product $(\mathbf{t}, r_\phi) \cdot (\mathbf{t}', r_{\phi'}) = (\mathbf{t} + r_\phi \mathbf{t}', r_{\phi+\phi'})$.
- $SE(2)$ is the principal bundle associated with $R \times \mathbb{P}^1$: $\mathbb{R}^2 \simeq SE(2)/SO(2)$.
- Then ω is invariant under the action of $SE(2)$ on $T(\mathbb{R}^2 \times SO(2))$: any two horizontal planes in $\mathbb{R}^2 \times SO(2)$ can be equivariantly identified by a suitable displacement.

  The distribution of horizontal planes realizes a connection in $R \times SO(2)$, allowing for parallel transport, covariant derivation...
- The long-range connections in $V1$ implement these contact structure and connection.
- Application to illusory contours: minimize distance in the subriemannian metric defined by the horizontal planes in the fiber bundle (Citti & Sarti, Petitot 2003).
- The $SE(2)$ equivariant structure is also fundamental to the problem of visual hallucinations as we shall see next...

Geometric hallucinations as a spontaneous activity in $V1$

Various types of non optical stimulation of the brain can induce visual hallucinatory patterns. Examples under marijuana or LSD:

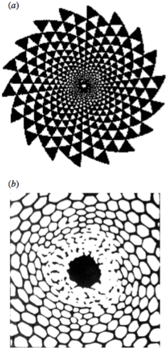

Figure 1. (a) 'Phosphene' produced by deep binocular pressure on the eyeballs. Redrawn from Tyler (1978). (b) Honeycomb hallucination generated by marijuana. Redrawn from Clottes & Lewis-Williams (1998).

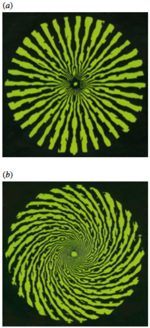

Figure 2. (a) Funnel and (b) spiral hallucinations generated by LSD. Redrawn from Oster (1970).

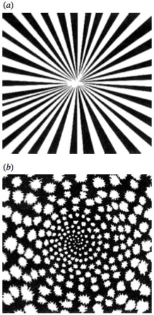

Figure 3. (a) Funnel and (b) spiral tunnel hallucinations generated by LSD. Redrawn from Siegel (1977).

(from Bressloff et al 2001)

The "ring model" of Bressloff, Cowan, Golubitsky

The "ring model" of Bressloff, Cowan, Golubitsky

Wilson-Cowan equation for the averaged action potential a of neural field:

$$(*)\ \ \frac{da(\mathbf{x},\theta,t)}{dt} = -a(\mathbf{x},\theta,t) + \int_{\mathbb{R}^2}\int_0^\pi w(\mathbf{x},\theta;\mathbf{x}',\theta')S(a(\mathbf{x}',\theta',t))d\theta' d\mathbf{x}' + I_{ext}$$

S = sigmoid function, $S(0)=0$, $S'(0)=\mu$ (bifurcation parameter).
$I_{ext}=0$ (no external input), w = synaptic strength between neurons.

The "ring model" of Bressloff, Cowan, Golubitsky

Wilson-Cowan equation for the averaged action potential a of neural field:

$$(*)\ \frac{da(\mathbf{x},\theta,t)}{dt} = -a(\mathbf{x},\theta,t) + \int_{\mathbb{R}^2}\int_0^{\pi} w(\mathbf{x},\theta;\mathbf{x}',\theta')S(a(\mathbf{x}',\theta',t))d\theta' d\mathbf{x}' + I_{ext}$$

S = sigmoid function, $S(0) = 0$, $S'(0) = \mu$ (bifurcation parameter).
$I_{ext} = 0$ (no external input), w = synaptic strength between neurons.

The contact structure of $V1$ must be encoded in the function w:

- $w(\mathbf{x},\theta;\mathbf{x}',\theta') = w_{loc}(\theta,\theta') + \beta w_{lat}(\mathbf{x},\theta;\mathbf{x}',\theta')$ (β = relative strength of loc and lat connections).

The "ring model" of Bressloff, Cowan, Golubitsky

Wilson-Cowan equation for the averaged action potential a of neural field:

$$(*)\ \ \frac{da(\mathbf{x},\theta,t)}{dt} = -a(\mathbf{x},\theta,t) + \int_{\mathbb{R}^2}\int_0^\pi w(\mathbf{x},\theta;\mathbf{x}',\theta')S(a(\mathbf{x}',\theta',t))d\theta' d\mathbf{x}' + I_{ext}$$

S = sigmoid function, $S(0) = 0$, $S'(0) = \mu$ (bifurcation parameter).
$I_{ext} = 0$ (no external input), w = synaptic strength between neurons.

The contact structure of $V1$ must be encoded in the function w:

- $w(\mathbf{x},\theta;\mathbf{x}',\theta') = w_{loc}(\theta,\theta') + \beta w_{lat}(\mathbf{x},\theta;\mathbf{x}',\theta')$ (β = relative strength of loc and lat connections).
- Local connections: $w_{loc} = g(|\theta-\theta'|)$, π-periodic.

The "ring model" of Bressloff, Cowan, Golubitsky

Wilson-Cowan equation for the averaged action potential a of neural field:

$$(*)\ \frac{da(\mathbf{x},\theta,t)}{dt} = -a(\mathbf{x},\theta,t) + \int_{\mathbb{R}^2}\int_0^\pi w(\mathbf{x},\theta;\mathbf{x}',\theta')S(a(\mathbf{x}',\theta',t))d\theta' d\mathbf{x}' + I_{ext}$$

S = sigmoid function, $S(0) = 0$, $S'(0) = \mu$ (bifurcation parameter).
$I_{ext} = 0$ (no external input), w = synaptic strength between neurons.

The contact structure of $V1$ must be encoded in the function w:

- $w(\mathbf{x},\theta;\mathbf{x}',\theta') = w_{loc}(\theta,\theta') + \beta w_{lat}(\mathbf{x},\theta;\mathbf{x}',\theta')$ (β = relative strength of loc and lat connections).
- Local connections: $w_{loc} = g(|\theta-\theta'|)$, π-periodic.
- Long range connections: $w_{lat} = h(\|\mathbf{x}-\mathbf{x}'\|)\delta(r_{-\theta}[\mathbf{x}-\mathbf{x}']\cdot\mathbf{e}_2)\delta(\theta-\theta')$ where h is a difference of Gaussian functions (empirical approx.).

The "ring model" of Bressloff, Cowan, Golubitsky

Wilson-Cowan equation for the averaged action potential a of neural field:

$$(*) \quad \frac{da(\mathbf{x},\theta,t)}{dt} = -a(\mathbf{x},\theta,t) + \int_{\mathbb{R}^2}\int_0^{\pi} w(\mathbf{x},\theta;\mathbf{x}',\theta')S(a(\mathbf{x}',\theta',t))d\theta' d\mathbf{x}' + I_{ext}$$

S = sigmoid function, $S(0) = 0$, $S'(0) = \mu$ (bifurcation parameter).
$I_{ext} = 0$ (no external input), w = synaptic strength between neurons.

The contact structure of $V1$ must be encoded in the function w:

- $w(\mathbf{x},\theta;\mathbf{x}',\theta') = w_{loc}(\theta,\theta') + \beta w_{lat}(\mathbf{x},\theta;\mathbf{x}',\theta')$ (β = relative strength of loc and lat connections).
- Local connections: $w_{loc} = g(|\theta-\theta'|)$, π-periodic.
- Long range connections: $w_{lat} = h(\|\mathbf{x}-\mathbf{x}'\|)\delta(r_{-\theta}[\mathbf{x}-\mathbf{x}']\cdot\mathbf{e}_2)\delta(\theta-\theta')$ where h is a difference of Gaussian functions (empirical approx.).

Remarks

1. $a = 0$ is the basic state, stable if μ is small enough.
2. Eq. $(*)$ is invariant under all isometries in $\mathbb{R}^2 \times \mathbb{S}^1$: group $E(2)$ generated by $SE(2)$ and the reflection $(\kappa\mathbf{x}, -\theta)$.

Sketch of the bifurcation analysis ("à la Turing")

Sketch of the bifurcation analysis ("à la Turing")

1. Linear stability of $a = 0$: Fourier and perturbation analysis of $\sigma a = -a + \mu w * a$ ($w = w_{loc} + \beta w_{lat}$, $\beta << 1$).
   Critical modes with wavelength k_c are activated at $\mu = \mu_c$.

Sketch of the bifurcation analysis ("à la Turing")

1. Linear stability of $a = 0$: Fourier and perturbation analysis of $\sigma a = -a + \mu w * a$ ($w = w_{loc} + \beta w_{lat}$, $\beta << 1$).
   Critical modes with wavelength k_c are activated at $\mu = \mu_c$.
2. Look for spatially periodic solutions: invariant under translations on a periodic lattice $\mathcal{L} \simeq \mathbb{Z}^2 \Rightarrow$ compact domain $\mathbb{R}^2/\mathcal{L} \simeq \mathbb{T}^2$ and compact symmetry group $G \simeq D_m \ltimes \mathbb{R}^2/\mathbb{Z}^2$ where $m = 2$ (rhombic lattice), 4 (square lattice) or 6 (hexagonal lattice).

Sketch of the bifurcation analysis ("à la Turing")

1. Linear stability of $a = 0$: Fourier and perturbation analysis of $\sigma a = -a + \mu w * a$ ($w = w_{loc} + \beta w_{lat}$, $\beta << 1$).
   Critical modes with wavelength k_c are activated at $\mu = \mu_c$.
2. Look for spatially periodic solutions: invariant under translations on a periodic lattice $\mathcal{L} \simeq \mathbb{Z}^2 \Rightarrow$ compact domain $\mathbb{R}^2/\mathcal{L} \simeq \mathbb{T}^2$ and compact symmetry group $G \simeq D_m \ltimes \mathbb{R}^2/\mathbb{Z}^2$ where $m = 2$ (rhombic lattice), 4 (square lattice) or 6 (hexagonal lattice).
3. Critical eigenfunctions $\psi_j = u(\theta)e^{\pm i\mathbf{k}_j \cdot \mathbf{x}}$ with $u(\theta) = u(\theta + \pi)$ and

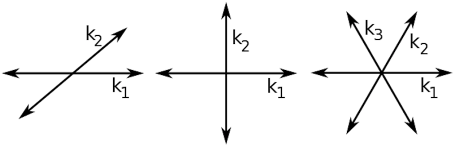

Sketch of the bifurcation analysis ("à la Turing")

1. Linear stability of $a = 0$: Fourier and perturbation analysis of $\sigma a = -a + \mu w * a$ ($w = w_{loc} + \beta w_{lat}$, $\beta << 1$).
   Critical modes with wavelength k_c are activated at $\mu = \mu_c$.
2. Look for spatially periodic solutions: invariant under translations on a periodic lattice $\mathcal{L} \simeq \mathbb{Z}^2 \Rightarrow$ compact domain $\mathbb{R}^2/\mathcal{L} \simeq \mathbb{T}^2$ and compact symmetry group $G \simeq D_m \ltimes \mathbb{R}^2/\mathbb{Z}^2$ where $m = 2$ (rhombic lattice), 4 (square lattice) or 6 (hexagonal lattice).
3. Critical eigenfunctions $\psi_j = u(\theta)e^{\pm i\mathbf{k}_j \cdot \mathbf{x}}$ with $u(\theta) = u(\theta + \pi)$ and

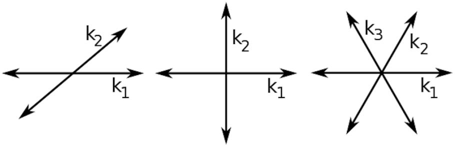

4. Remark: the cases $u(\theta) = \pm u(-\theta)$ (scalar field or pseudoscalar field) can occur. They lead to different bifurcation diagrams (see B-Vivancos, C. & Melbourne 1994).

Hallucinations as retinotopic images of bifurcated patterns in $V1$

Equivariant bifurcation theory applies and leads to classification of bifurcated states w.r.t. residual symmetry (isotropy).

At first order $a_\mu(\mathbf{x}, \theta) \sim \sum z_j(\mu)\psi_j + c.c.$

Examples

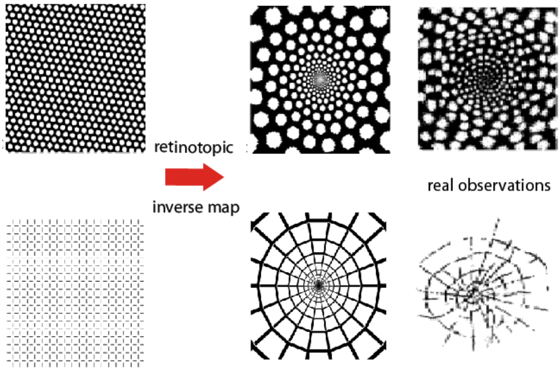

Extending the model: $V1$ as a structure tensor processor

To improve the "ring model" O. Faugeras and P.C. (Plos Comp Bio 2009) assumed that neurons are sensitive to the structure tensor of the image intensity, which is known to be a good detector for image textures.

Extending the model: $V1$ as a structure tensor processor

To improve the "ring model" O. Faugeras and P.C. (Plos Comp Bio 2009) assumed that neurons are sensitive to the structure tensor of the image intensity, which is known to be a good detector for image textures.

This model was studied in a series of papers with Gregory Faye (CNRS, U. of Toulouse), see his thesis on tel.archives-ouvertes.fr.

Extending the model: $V1$ as a structure tensor processor

To improve the "ring model" O. Faugeras and P.C. (Plos Comp Bio 2009) assumed that neurons are sensitive to the structure tensor of the image intensity, which is known to be a good detector for image textures.

This model was studied in a series of papers with Gregory Faye (CNRS, U. of Toulouse), see his thesis on tel.archives-ouvertes.fr.

Next I introduce the model and its main features.

In the last part of the talk I will show how this leads to a problem of pattern formation in the hyperbolic plane and how this was tackled.

The structure tensor as a texture detector

Let $g_\sigma(x,y) = \frac{1}{2\pi\sigma_1^2}\exp(-(x^2+y^2)/2\sigma^2)$.
For the image intensity $I(x,y)$ we set $I_{\sigma_1} = I * g_{\sigma_1}$.

The structure tensor as a texture detector

Let $g_\sigma(x,y) = \frac{1}{2\pi\sigma_1^2}\exp(-(x^2+y^2)/2\sigma^2)$.
For the image intensity $I(x,y)$ we set $I_{\sigma_1} = I * g_{\sigma_1}$.

The structure tensor of the image is the matrix

$$\mathcal{T}(x,y) = g_{\sigma_2} * \left(\nabla I_{\sigma_1} \nabla^T I_{\sigma_1}\right)$$

σ_2 defines the characteristic size of the texture to be represented.

The structure tensor as a texture detector

Let $g_\sigma(x, y) = \frac{1}{2\pi\sigma_1^2} \exp(-(x^2 + y^2)/2\sigma^2)$.

For the image intensity $I(x, y)$ we set $I_{\sigma_1} = I * g_{\sigma_1}$.

The structure tensor of the image is the matrix

$$\mathcal{T}(x, y) = g_{\sigma_2} * \left(\nabla I_{\sigma_1} \nabla^T I_{\sigma_1}\right)$$

σ_2 defines the characteristic size of the texture to be represented.

$\mathcal{T}$ is a symmetric positive definite matrix: $\{\mathcal{T}\} \simeq \mathrm{SPD}(2)$.

This object was introduced in computer vision as a local descriptor for edges, corners and contrast of images.

We shall assume that structure tensors are encoded in the hypercolumns of $V1$, so that $V1 \simeq \mathbb{R}^2 \times \mathrm{SPD}(2)$.

How does this improve the orientation model, and is it a natural assumption?

Basic properties of the structure tensor

Basic properties of the structure tensor

$\mathcal{T}$ has two real eigenvalues: $\lambda_1 \geq \lambda_2 > 0$ with eigenvectors $\mathbf{e}_1 \perp \mathbf{e}_2$.
Elementary algebra shows $\mathcal{T} = (\lambda_1 - \lambda_2)\mathbf{e}_1\mathbf{e}_1^T + \lambda_2\mathbf{I}_2$.

Basic properties of the structure tensor

$\mathcal{T}$ has two real eigenvalues: $\lambda_1 \geq \lambda_2 > 0$ with eigenvectors $\mathbf{e}_1 \perp \mathbf{e}_2$.
Elementary algebra shows $\mathcal{T} = (\lambda_1 - \lambda_2)\mathbf{e}_1\mathbf{e}_1^T + \lambda_2 \mathbf{I}_2$.

- $\lambda_1 \approx \lambda_2 \Rightarrow$ isotropic image
- $\lambda_1 \gg \lambda_2 \approx 0 \Rightarrow$ straight edge along $\mathbf{e}_2$
- $\lambda_1 \geq \lambda_2 \gg 0 \Rightarrow$ corner
- the size of λ_j defines the contrast along $\mathbf{e}_j$

the ellipse $\mathbf{x}\mathcal{T}\mathbf{x}^T = 1$

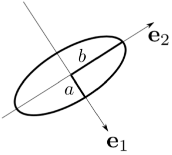

$a = \sqrt{\lambda_1}$, $b = \sqrt{\lambda_2}$

Basic properties of the structure tensor

$\mathcal{T}$ has two real eigenvalues: $\lambda_1 \geq \lambda_2 > 0$ with eigenvectors $\mathbf{e}_1 \perp \mathbf{e}_2$.
Elementary algebra shows $\mathcal{T} = (\lambda_1 - \lambda_2)\mathbf{e}_1\mathbf{e}_1^T + \lambda_2\mathbf{I}_2$.

- $\lambda_1 \approx \lambda_2 \Rightarrow$ isotropic image
- $\lambda_1 \gg \lambda_2 \approx 0 \Rightarrow$ straight edge along $\mathbf{e}_2$
- $\lambda_1 \geq \lambda_2 \gg 0 \Rightarrow$ corner
- the size of λ_j defines the contrast along $\mathbf{e}_j$

the ellipse $\mathbf{x}\mathcal{T}\mathbf{x}^T = 1$

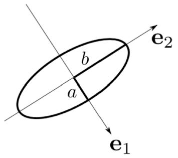

$a = \sqrt{\lambda_1}$, $b = \sqrt{\lambda_2}$

Let $\mathbf{e}_2 = (r\cos\theta, r\sin\theta)$, θ defines the preferred orientation of the neuron.
Note that $\mathcal{T}$ is invariant under $\theta \to \theta + \pi$.

Basic properties of the structure tensor

$\mathcal{T}$ has two real eigenvalues: $\lambda_1 \geq \lambda_2 > 0$ with eigenvectors $\mathbf{e}_1 \perp \mathbf{e}_2$.
Elementary algebra shows $\mathcal{T} = (\lambda_1 - \lambda_2)\mathbf{e}_1\mathbf{e}_1^T + \lambda_2 \mathbf{I}_2$.

- $\lambda_1 \approx \lambda_2 \Rightarrow$ isotropic image
- $\lambda_1 \gg \lambda_2 \approx 0 \Rightarrow$ straight edge along $\mathbf{e}_2$
- $\lambda_1 \geq \lambda_2 \gg 0 \Rightarrow$ corner
- the size of λ_j defines the contrast along $\mathbf{e}_j$

the ellipse $\mathbf{x}\mathcal{T}\mathbf{x}^T = 1$

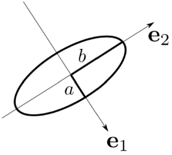

$a = \sqrt{\lambda_1}$, $b = \sqrt{\lambda_2}$

Let $\mathbf{e}_2 = (r\cos\theta, r\sin\theta)$, θ defines the preferred orientation of the neuron.
Note that $\mathcal{T}$ is invariant under $\theta \to \theta + \pi$.

In the limit $\lambda_2 = 0$ one recovers the ring model + the contrast along $\mathbf{e}_1$.

Basic properties of the structure tensor

$\mathcal{T}$ has two real eigenvalues: $\lambda_1 \geq \lambda_2 > 0$ with eigenvectors $\mathbf{e}_1 \perp \mathbf{e}_2$.
Elementary algebra shows $\mathcal{T} = (\lambda_1 - \lambda_2)\mathbf{e}_1\mathbf{e}_1^T + \lambda_2\mathbf{I}_2$.

- $\lambda_1 \approx \lambda_2 \Rightarrow$ isotropic image
- $\lambda_1 \gg \lambda_2 \approx 0 \Rightarrow$ straight edge along $\mathbf{e}_2$
- $\lambda_1 \geq \lambda_2 \gg 0 \Rightarrow$ corner
- the size of λ_j defines the contrast along $\mathbf{e}_j$

the ellipse $\mathbf{x}\mathcal{T}\mathbf{x}^T = 1$

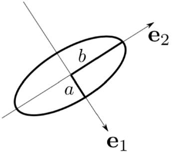

$a = \sqrt{\lambda_1}$, $b = \sqrt{\lambda_2}$

Let $\mathbf{e}_2 = (r\cos\theta, r\sin\theta)$, θ defines the preferred orientation of the neuron.
Note that $\mathcal{T}$ is invariant under $\theta \to \theta + \pi$.

In the limit $\lambda_2 = 0$ one recovers the ring model + the contrast along $\mathbf{e}_1$.

There are some biological arguments supporting this model for $V1$ (but experimental confirmation is missing).

Riemannian geometry on the set of structure tensors

$\mathrm{SPD}(2) \simeq \mathrm{Q}^+ =$ space of positive definite quadratic forms $\mathbf{x}\mathcal{T}\mathbf{x}^T$ in $\mathbb{R}^2$.

Riemannian geometry on the set of structure tensors

$\mathrm{SPD}(2) \simeq \mathrm{Q}^+ =$ space of positive definite quadratic forms $\mathbf{x}\mathcal{T}\mathbf{x}^T$ in $\mathbb{R}^2$.

It is natural to take the metric on $\mathrm{SPD}(2)$ such that changes of coordinates in Q^+ leave distances invariant.

Riemannian geometry on the set of structure tensors

$\mathrm{SPD}(2) \simeq \mathrm{Q}^+ =$ space of positive definite quadratic forms $\mathbf{x}\mathcal{T}\mathbf{x}^T$ in $\mathbb{R}^2$.

It is natural to take the metric on $\mathrm{SPD}(2)$ such that changes of coordinates in Q^+ leave distances invariant.

The following formulation is equivalent and more convenient for our purpose:

$\mathcal{T} = \Delta\widetilde{\mathcal{T}}$ where $\det\widetilde{\mathcal{T}} = 1$. It follows that $\mathrm{SPD}(2) = \mathbb{R}_*^+ \times \mathrm{SSPD}(2)$.

Riemannian geometry on the set of structure tensors

$\mathrm{SPD}(2) \simeq \mathrm{Q}^+ =$ space of positive definite quadratic forms $\mathbf{x}\mathcal{T}\mathbf{x}^T$ in $\mathbb{R}^2$.

It is natural to take the metric on $\mathrm{SPD}(2)$ such that changes of coordinates in Q^+ leave distances invariant.

The following formulation is equivalent and more convenient for our purpose:

$\mathcal{T} = \Delta\widetilde{\mathcal{T}}$ where $\det\widetilde{\mathcal{T}} = 1$. It follows that $\mathrm{SPD}(2) = \mathbb{R}_*^+ \times \mathrm{SSPD}(2)$.

Now, $\mathrm{SSPD}(2) \simeq$ Lorentz surface $H^2 \simeq$ Poincaré disc $\mathbb{D} = \{z \in \mathbb{C}, |z| < 1\}$ (by a suitable stereographic projection,) so that $\mathrm{SPD}(2) \simeq \mathbb{R}_*^+ \times \mathbb{D}$.

Riemannian geometry on the set of structure tensors

$\mathrm{SPD}(2) \simeq \mathrm{Q}^+ =$ space of positive definite quadratic forms $\mathbf{x}\mathcal{T}\mathbf{x}^T$ in $\mathbb{R}^2$.

It is natural to take the metric on $\mathrm{SPD}(2)$ such that changes of coordinates in Q^+ leave distances invariant.

The following formulation is equivalent and more convenient for our purpose:

$\mathcal{T} = \Delta\widetilde{\mathcal{T}}$ where $\det\widetilde{\mathcal{T}} = 1$. It follows that $\mathrm{SPD}(2) = \mathbb{R}_*^+ \times \mathrm{SSPD}(2)$.

Now, $\mathrm{SSPD}(2) \simeq$ Lorentz surface $H^2 \simeq$ Poincaré disc $\mathbb{D} = \{z \in \mathbb{C}, |z| < 1\}$ (by a suitable stereographic projection,) so that $\mathrm{SPD}(2) \simeq \mathbb{R}_*^+ \times \mathbb{D}$.

This provides us with a metric on $\mathrm{SPD}(2)$, for which the distance is

$$d(\mathcal{T}, \mathcal{T}') = \sqrt{2\log^2(\frac{\Delta}{\Delta'}) + \operatorname{artanh}^2 \frac{|z - z'|}{|1 - \bar{z}z'|}}$$

Riemannian geometry on the set of structure tensors

$\mathrm{SPD}(2) \simeq \mathrm{Q}^+ =$ space of positive definite quadratic forms $\mathbf{x}\mathcal{T}\mathbf{x}^T$ in $\mathbb{R}^2$.

It is natural to take the metric on $\mathrm{SPD}(2)$ such that changes of coordinates in Q^+ leave distances invariant.

The following formulation is equivalent and more convenient for our purpose:

$\mathcal{T} = \Delta\widetilde{\mathcal{T}}$ where $\det\widetilde{\mathcal{T}} = 1$. It follows that $\mathrm{SPD}(2) = \mathbb{R}_*^+ \times \mathrm{SSPD}(2)$.

Now, $\mathrm{SSPD}(2) \simeq$ Lorentz surface $H^2 \simeq$ Poincaré disc $\mathbb{D} = \{z \in \mathbb{C}, |z| < 1\}$ (by a suitable stereographic projection,) so that $\mathrm{SPD}(2) \simeq \mathbb{R}_*^+ \times \mathbb{D}$.

This provides us with a metric on $\mathrm{SPD}(2)$, for which the distance is

$$d(\mathcal{T}, \mathcal{T}') = \sqrt{2\log^2\left(\frac{\Delta}{\Delta'}\right) + \operatorname{artanh}^2 \frac{|z - z'|}{|1 - \bar{z}z'|}}$$

The isometry group is now $\mathbb{R}_*^+ \times U(1,1)$, where $U(1,1)$ acts on $\mathbb{D}$ by

$$\gamma z = \frac{\alpha z + \beta}{\bar{\beta} z + \bar{\alpha}}\ ,\ |\alpha|^2 - |\beta|^2 = 1,\ \text{and reflection } \kappa z = \bar{z}.$$

Implementation of the structure tensor formalism in the analysis of spontaneous activity in $V1$

Implementation of the structure tensor formalism in the analysis of spontaneous activity in $V1$

- $V1 \simeq \mathbb{R}^2 \times \mathbb{R}_*^+ \times \mathbb{D}$ considered as a fiber bundle over $\mathbb{R}^2$.

Implementation of the structure tensor formalism in the analysis of spontaneous activity in $V1$

- $V1 \simeq \mathbb{R}^2 \times \mathbb{R}_*^+ \times \mathbb{D}$ considered as a fiber bundle over $\mathbb{R}^2$.
- Taking fibers $\mathbb{R}_*^+ \times \mathbb{D}$ makes analysis considerably more difficult than $\mathbb{S}^1$.

Implementation of the structure tensor formalism in the analysis of spontaneous activity in $V1$

- $V1 \simeq \mathbb{R}^2 \times \mathbb{R}_*^+ \times \mathbb{D}$ considered as a fiber bundle over $\mathbb{R}^2$.
- Taking fibers $\mathbb{R}_*^+ \times \mathbb{D}$ makes analysis considerably more difficult than $\mathbb{S}^1$.
- First step: suppose isolated hypercolumns and discard the $\mathbb{R}_*^+$ component.

Implementation of the structure tensor formalism in the analysis of spontaneous activity in $V1$

- $V1 \simeq \mathbb{R}^2 \times \mathbb{R}_*^+ \times \mathbb{D}$ considered as a fiber bundle over $\mathbb{R}^2$.
- Taking fibers $\mathbb{R}_*^+ \times \mathbb{D}$ makes analysis considerably more difficult than $\mathbb{S}^1$.
- First step: suppose isolated hypercolumns and discard the $\mathbb{R}_*^+$ component.
- This leads to the problem of bifurcation of patterns in $\mathbb{D}$, or equivalently in the hyperbolic plane.

Implementation of the structure tensor formalism in the analysis of spontaneous activity in $V1$

- $V1 \simeq \mathbb{R}^2 \times \mathbb{R}_*^+ \times \mathbb{D}$ considered as a fiber bundle over $\mathbb{R}^2$.
- Taking fibers $\mathbb{R}_*^+ \times \mathbb{D}$ makes analysis considerably more difficult than $\mathbb{S}^1$.
- First step: suppose isolated hypercolumns and discard the $\mathbb{R}_*^+$ component.
- This leads to the problem of bifurcation of patterns in $\mathbb{D}$, or equivalently in the hyperbolic plane.
- In the context of parabolic PDEs in $\mathbb{D}$, see my paper with G. Faye:

  Pattern formation for the Swift-Hohenberg equation on the hyperbolic plane, J. Dyn & Diff Eqs, Online First (2013).

Implementation of the structure tensor formalism in the analysis of spontaneous activity in $V1$

- $V1 \simeq \mathbb{R}^2 \times \mathbb{R}_*^+ \times \mathbb{D}$ considered as a fiber bundle over $\mathbb{R}^2$.
- Taking fibers $\mathbb{R}_*^+ \times \mathbb{D}$ makes analysis considerably more difficult than $\mathbb{S}^1$.
- First step: suppose isolated hypercolumns and discard the $\mathbb{R}_*^+$ component.
- This leads to the problem of bifurcation of patterns in $\mathbb{D}$, or equivalently in the hyperbolic plane.
- In the context of parabolic PDEs in $\mathbb{D}$, see my paper with G. Faye:

  Pattern formation for the Swift-Hohenberg equation on the hyperbolic plane, J. Dyn & Diff Eqs, Online First (2013).
- For an attempt to treat the "spatialized" system (extended to $\mathbb{R}^2$), see my paper with G. Faye in J. Networks & Heterogeneous Media, 2013.

Harmonic and spectral analysis in $\mathbb{D}$

Harmonic and spectral analysis in $\mathbb{D}$

- Subgroup of direct isometries (displacements) in $U(1,1)$: pseudo-unitary group $SU(1,1)$ acting in $\mathbb{D}$ by $\gamma z = \frac{\alpha z+\beta}{\bar{\beta} z+\bar{\alpha}}$, $|\alpha|^2 - |\beta|^2 = 1$.

Harmonic and spectral analysis in $\mathbb{D}$

- Subgroup of direct isometries (displacements) in $U(1,1)$: pseudo-unitary group $SU(1,1)$ acting in $\mathbb{D}$ by $\gamma z = \frac{\alpha z+\beta}{\bar{\beta} z+\bar{\alpha}}$, $|\alpha|^2 - |\beta|^2 = 1$.
- Iwasawa Theorem: $SU(1,1) = KAN$ were K, A, N are 1-parameter subgroups with orbits

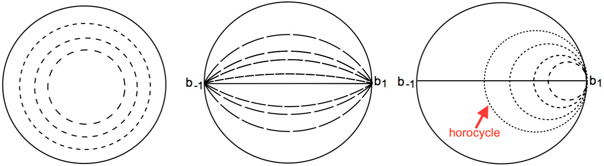

rotations hyperbolic boosts parabolic transformations

Harmonic and spectral analysis in $\mathbb{D}$

- Subgroup of direct isometries (displacements) in $U(1,1)$: pseudo-unitary group $SU(1,1)$ acting in $\mathbb{D}$ by $\gamma z = \frac{\alpha z+\beta}{\bar\beta z+\bar\alpha}$, $|\alpha|^2 - |\beta|^2 = 1$.
- Iwasawa Theorem: $SU(1,1) = KAN$ were K, A, N are 1-parameter subgroups with orbits

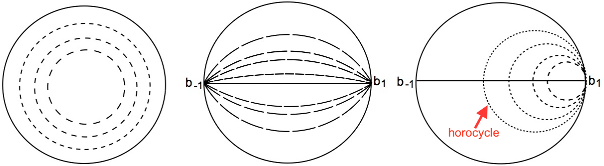

rotations hyperbolic boosts parabolic transformations

- Harmonic analysis in $\mathbb{D}$ (Fourier-Helgason): based on elementary eigenfunctions $e_{\rho,b}(z) = e^{(i\rho+\frac{1}{2})\langle z,b\rangle}$, $\rho \in \mathbb{C}$, where $b \in \partial\mathbb{D}$ and $\langle z,b\rangle$ is a distance built from horocycle based at b and passing by z.
  It satisfies $-\triangle_{\mathbb{D}}\, e_{\rho,b} = (\rho^2 + \frac{1}{4})e_{\rho,b}$.
  It allows to build a "Fourier transform" in $\mathbb{D}$ $\rightarrow$ spectral analysis.

Periodic pattern formation in the Poincaré disc (sketch)

Periodic pattern formation in the Poincaré disc (sketch)

- Let $\Gamma \subset SU(1,1)$ be a discrete subgroup which tiles $\mathbb{D}$ from a compact fundamental domain F_Γ (polygon).
  Then Γ is spanned by a finite number of hyperbolic boosts.
  Γ is called a cocompact Fuchsian (or lattice) group.

Periodic pattern formation in the Poincaré disc (sketch)

- Let $\Gamma \subset SU(1,1)$ be a discrete subgroup which tiles $\mathbb{D}$ from a compact fundamental domain F_Γ (polygon).
  Then Γ is spanned by a finite number of hyperbolic boosts.
  Γ is called a cocompact Fuchsian (or lattice) group.
- $\mathbb{D}/\Gamma \simeq$ compact Riemann surface of genus $g \geq 2$ (a torus with g holes).
  $\simeq$ polygon F_Γ with opposite sides identified by periodicity.

Periodic pattern formation in the Poincaré disc (sketch)

- Let $\Gamma \subset SU(1,1)$ be a discrete subgroup which tiles $\mathbb{D}$ from a compact fundamental domain F_Γ (polygon).
  Then Γ is spanned by a finite number of hyperbolic boosts.
  Γ is called a cocompact Fuchsian (or lattice) group.
- $\mathbb{D}/\Gamma \simeq$ compact Riemann surface of genus $g \geq 2$ (a torus with g holes).
  $\simeq$ polygon F_Γ with opposite sides identified by periodicity.
- The $U(1,1)$-invariant equation projects onto $\mathbb{D}/\Gamma$ to a G_Γ-invariant equation where G_Γ is the symmetry group of F_Γ (seen as a g-torus).

Periodic pattern formation in the Poincaré disc (sketch)

- Let $\Gamma \subset SU(1,1)$ be a discrete subgroup which tiles $\mathbb{D}$ from a compact fundamental domain F_Γ (polygon).
  Then Γ is spanned by a finite number of hyperbolic boosts.
  Γ is called a cocompact Fuchsian (or lattice) group.
- $\mathbb{D}/\Gamma \simeq$ compact Riemann surface of genus $g \geq 2$ (a torus with g holes).
  $\simeq$ polygon F_Γ with opposite sides identified by periodicity.
- The $U(1,1)$-invariant equation projects onto $\mathbb{D}/\Gamma$ to a G_Γ-invariant equation where G_Γ is the symmetry group of F_Γ (seen as a g-torus).
- G_Γ is a finite group $\rightarrow$ finite dimensional irreducible representations.
  Hence standard techniques (center manifold theorem) apply to reduce the bifurcation problem to one in a finite dimensional space (irrep of G_Γ).

Periodic pattern formation in the Poincaré disc (sketch)

- Let $\Gamma \subset SU(1,1)$ be a discrete subgroup which tiles $\mathbb{D}$ from a compact fundamental domain F_Γ (polygon).
  Then Γ is spanned by a finite number of hyperbolic boosts.
  Γ is called a cocompact Fuchsian (or lattice) group.
- $\mathbb{D}/\Gamma \simeq$ compact Riemann surface of genus $g \geq 2$ (a torus with g holes).
  $\simeq$ polygon F_Γ with opposite sides identified by periodicity.
- The $U(1,1)$-invariant equation projects onto $\mathbb{D}/\Gamma$ to a G_Γ-invariant equation where G_Γ is the symmetry group of F_Γ (seen as a g-torus).
- G_Γ is a finite group $\rightarrow$ finite dimensional irreducible representations. Hence standard techniques (center manifold theorem) apply to reduce the bifurcation problem to one in a finite dimensional space (irrep of G_Γ).
- For a given Γ the area of a fundamental region is fixed (by Gauss-Bonnet formula) $\rightarrow$ no scale equivalence between lattices as in Euclidean plane.
- There are an infinite number of lattices in $\mathbb{D}$.

Periodic patterns with a regular octagonal domain F_Γ

This is the simplest example of a lattice on $\mathbb{D}$.

- The regular octagonal lattice group Γ is generated by four hyperbolic boosts.
- Vertex angles $\pi/8$, area 4π.
- $\mathbb{D}/\Gamma \simeq$ double torus (genus 2).
- $G_\Gamma = G_0 \cup \kappa G_0$ where $\kappa : z \to \bar{z}$ and $G_0 \simeq GL(2,3)$ ($|G_0| = 48$).

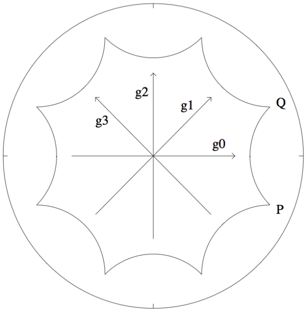

Periodic patterns with a regular octagonal domain F_Γ

This is the simplest example of a lattice on $\mathbb{D}$.

- The regular octagonal lattice group Γ is generated by four hyperbolic boosts.
- Vertex angles $\pi/8$, area 4π.
- $\mathbb{D}/\Gamma \simeq$ double torus (genus 2).
- $G_\Gamma = G_0 \cup \kappa G_0$ where $\kappa : z \to \bar{z}$ and $G_0 \simeq GL(2,3)$ ($|G_0| = 48$).

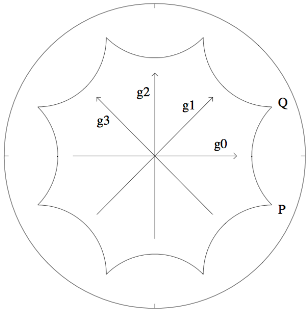

- 13 irreducible representations of $G_{\Gamma_O} \to$ 13 different bifurcation problems: 4 with dim 1, 2 with dim 2, 4 with dim 3 and 3 with dim 4.
- All "generic" bifurcating patterns have been described in Faye & C. 2011.

An example with a 1-dim. representation of G_Γ

This is the axis of Γ-periodic states which are invariant under the 48-element subgroup of G_Γ generated by $SL(2,3) = \{g \in GL(2,3) \mid \det(g) = 1\}$ and a reflection. Bifurcation is pitchfork.

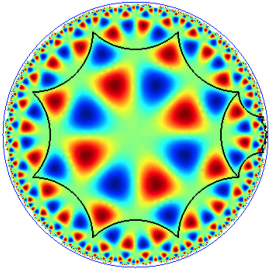

An example with a 1-dim. representation of G_Γ

This is the axis of Γ-periodic states which are invariant under the 48-element subgroup of G_Γ generated by $SL(2,3) = \{g \in GL(2,3) \mid \det(g) = 1\}$ and a reflection. Bifurcation is pitchfork.

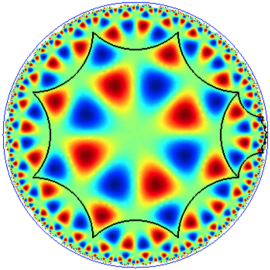

Remark: the numerical computation of Γ-periodic hyperbolic harmonics is tricky. There is no explicit formula (unlike in Euclidean case). Need to decompose F_Γ in fundamental triangles tiling it by reflections, then apply finite elements numerical schemes.

Bon anniversaire Jean-Marc!